Design and analysis of photonic crystal coupled cavity arrays for quantum simulation

Arka Majumdar,[1,*] Armand Rundquist,[1] Michal Bajcsy,[1] Vaishno D. Dasika,[2] Seth R. Bank,[2] and Jelena Vučković[1]
[1]*E. L. Ginzton Laboratory, Stanford University, Stanford, California 94305, USA*
[2]*Microelectronics Research Center, University of Texas, Austin, Texas 78712, USA*
(Received 13 September 2012; revised manuscript received 14 October 2012; published 19 November 2012)

We performed an experimental study of coupled optical cavity arrays in a photonic crystal platform. We find that the coupling between the cavities is significantly larger than the fabrication-induced disorder in the cavity frequencies. Satisfying this condition is necessary for using such cavity arrays to generate strongly correlated photons, which has potential application in the quantum simulation of many-body systems.

DOI: 10.1103/PhysRevB.86.195312 PACS number(s): 42.70.Qs, 42.50.Pq, 42.82.Et

I. INTRODUCTION

Solving strongly correlated quantum many-body systems is a formidable task. One promising approach is to mimic such complicated systems using another simpler and easily controllable quantum system, as envisioned by Feynman.[1] To that end, the first demonstration of quantum phase transitions with ultracold atoms in an optical lattice[2] sparked a significant amount of research on quantum simulation with atomic systems.[3] Another very promising direction of using photons themselves as the interacting particles has generated considerable interest recently.[4–6] The main idea of this approach is to obtain a correlated "quantum fluid of light"[4] by building a coupled network of nonlinear electromagnetic cavities. The photons can hop between cavities due to the electromagnetic coupling and can repel each other in the same cavity due to the intracavity nonlinearity. We note that such a coupled cavity network exhibits rich physics such as topologically protected optical delays,[7] even without any nonlinearity, although having nonlinear cavities opens up many more avenues of research. Obviously, the optical nonlinearity required for significant repulsion at low photon number is very high, and in current technology, only two-level systems [for example, atoms, single quantum emitters such as quantum dots (QDs), or superconducting transmon qubits] strongly coupled to a cavity provide such strong nonlinearity in the photon blockade regime.[8–11] In most of the applications relating to quantum simulations, one needs to deterministically position single quantum emitters in each of the cavities, which is very difficult to achieve with the state-of-the-art solid-state technology. However, recently several groups have demonstrated deterministic positioning of semiconductor QDs,[12–16] and the hope is that these site-controlled QDs will also perform well within the setting of cavity quantum electrodynamics (CQED). Another approach would be to use a bulk nonlinearity or quantum-well nonlinearity, but significantly enhanced by a cavity with a high-quality (Q) factor and low mode volume.[17,18] We note that such a platform consisting of coupled nonlinear cavities is useful not just for the quantum simulation but also for quantum error correction,[19] as well as for classical optical signal processing.[20]

Although plenty of theoretical proposals for simulating interesting physics in such a coupled cavity array (CCA) are present in the literature, the experimental progress in that direction is rather limited. As one needs to have many cavities for this operation, a solid-state system is obviously an ideal choice. However, due to imperfect nanofabrication, solid-state cavities have inherent disorder, resulting in different resonance frequencies than the cavities were originally designed for. Such disorder might limit the utility of CCAs for quantum simulation. However, in a recent paper it is argued that as long as the coupling strengths are much larger than the disorder, the CCAs can be used for quantum simulation, and it is shown that microwave transmission line cavities for circuit QED satisfy this condition.[21]

In this paper, we demonstrate high-Q two-dimensional (2D) CCAs based on photonic crystals fabricated in GaAs with embedded high-density self-assembled epitaxially grown InAs QDs. Although a pair of coupled cavities, also known as a photonic molecule, has been well studied in the literature,[22–27] relatively little literature exists for CCAs. A 2D CCA of photonic crystals in GaAs (with multiple quantum wells as active materials) has been studied previously for increasing the output light intensity from nanolasers or slowing down light,[28–31] but the Q factors of the cavities were too low to identify individual cavity modes. A long chain of high-Q coupled cavities has been studied in silicon,[32] but the physical phenomena observable in such a 1D chain are rather limited. While a 1D array[33] has been studied as a platform to simulate the physics of Bose glass[34] and Tonks-Girardeau gas,[35] a 2D array is a more suitable candidate for simulating many other systems, including topologically nontrivial states such as the fractional quantum Hall state.[36–38] We also note that, although an extensive treatment of such disorder in the context of circuit quantum electrodynamics has already been reported in Ref. 21, our optical cavity QED system is capable of achieving much larger coupling strengths (∼THz) between the cavities. We believe that our experimental findings (on the nature of coupling strengths and disorder) will provide a more realistic picture for exploring the utility of optical CCAs for quantum simulation.

II. SPECTRA OF COUPLED CAVITIES

In our experiment, we employ an array of linear three-hole ($L3$) defect photonic crystal cavities, typically studied in single QD-cavity QED experiments.[39,40] The fundamental mode of such a cavity is linearly polarized in the direction orthogonal to the cavity axis; in our proposed CCA geometry, all the cavities have parallel axes, and their modes have the same polarization. The photonic crystal CCA (with photonic crystal hole radius ∼60 nm and lattice periodicity 246 nm)

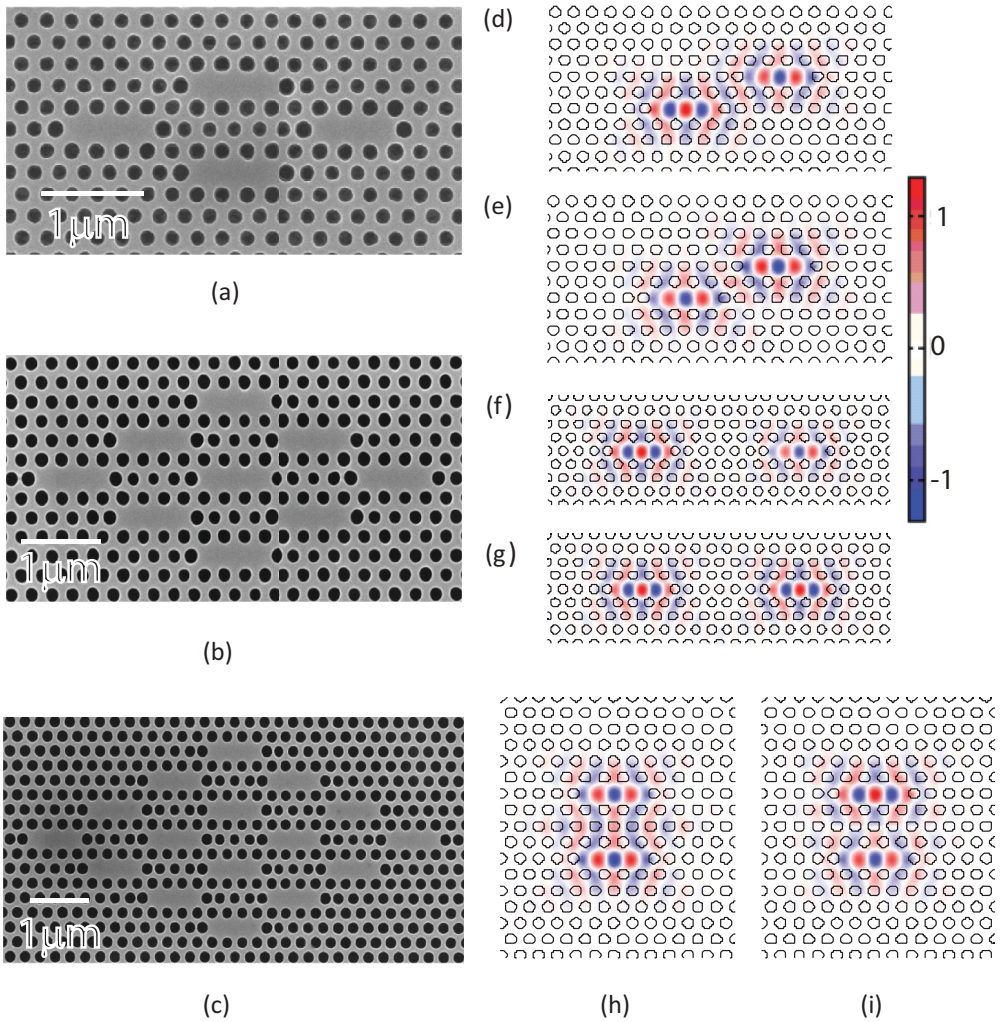

FIG. 1. (Color online) Scanning electron micrograph (SEM) images of CCA with (a) 4 cavities, (b) 9 cavities, and (c) 16 cavities. The simulated electric field profiles for each of the two supermodes of the coupled cavities are shown: (d), (e) for 60° coupled cavities; (f), (g) for laterally coupled cavities; (h), (i) for vertically coupled cavities.

is fabricated in a 164-nm-thick GaAs membrane (with self-assembled InAs QDs embedded at a depth of 82 nm from the surface) using electron-beam lithography and reactive ion etching.[39] Scanning electron micrographs of the fabricated structures are shown in Figs. 1(a)–1(c). Three different CCAs are designed consisting of 4, 9, and 16 cavities. These cavities are coupled to each other by three different coupling strengths depending on the relative orientation and separation of two cavities. When two cavities are coupled at an angle of 60° [Figs. 1(d) and 1(e)], the coupling strength t is strongest; for vertically stacked coupled cavities [Figs. 1(h) and 1(i)], the coupling strength J_1 is smaller than t; and for horizontal coupled cavities [Figs. 1(f) and 1(g)], the coupling strength J_2 is much smaller than t and J_1 (the difference in coupling strengths is a result of the different radiation patterns of the cavity modes and their different overlaps in various directions). From the finite-difference time domain (FDTD) simulations, we can calculate the field profiles of the coupled cavities [Figs. 1(d)–1(i)] and estimate the coupling strengths from the separation of the supermodes in the simulated spectra, assuming cavity operation in the range of QD emission (∼900–930 nm). For a hole radius r varying from 70 nm down to 50 nm, with photonic crystal lattice constant $a = 246$ nm, we find that $t/2\pi \sim 0.8$–1.3 THz, $J_1/2\pi \sim 0.4$–0.8 THz, and $J_2 \ll t, J_1$.

We characterize the resonances of the coupled cavity array by photoluminescence (PL) studies, where the large density of embedded QDs ($\sim 200/\mu m^2$) acts as an internal light source. Figures 2(a)–2(c) show the PL spectra obtained from the CCAs at 30 K, under excitation of an 820 nm continuous-wave excitation. The excitation power is ∼1 nW measured in front of the objective lens. Figure 2(d) shows the PL spectrum collected from the bulk QDs. The quality factors of the observed modes are ∼1000–3000 [Fig. 2(e)], and all the modes are linearly polarized with a similar polarization axis. We note that the set of higher Q-factor resonances in Fig. 2 is identified as the coupled fundamental modes of the $L3$ cavities, shown in Fig. 1. These modes are not necessarily in the same wavelength range for different sizes of the arrays, as the structures were defined during the fabrication process with different doses in e-beam lithography, and thus photonic crystals have different parameters (in this case slightly different radii).

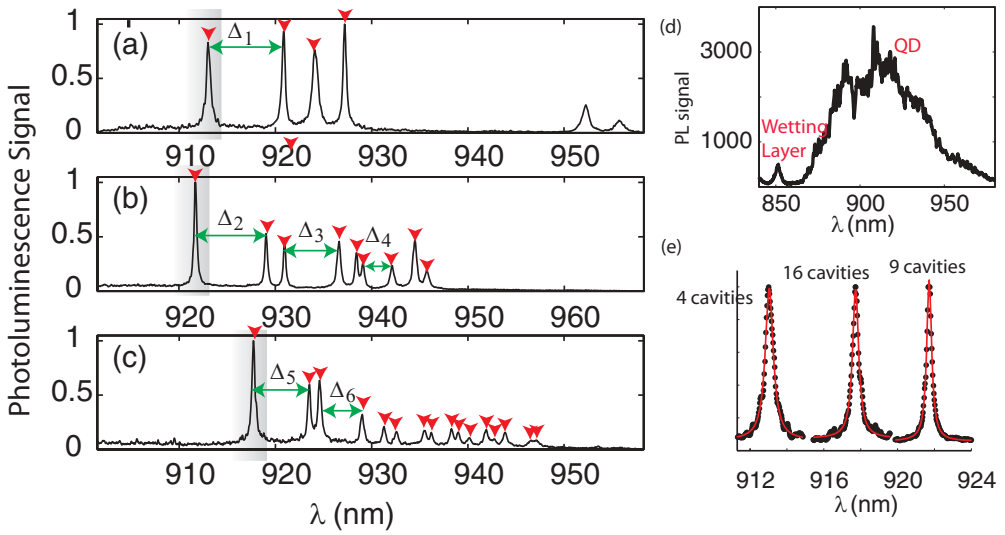

FIG. 2. (Color online) The PL spectra of the CCA for (a) 4, (b) 9, and (c) 16 cavities. We can clearly identify all the cavity array modes. We focus on several specific separations between the CCA modes labeled Δ_1 through Δ_6 in the plots and perform statistical analysis. We also observed several low-Q modes at long wavelengths for several cavity arrays, as can be seen in part (a). These modes are not the actual coupled cavity modes under study, which is confirmed by monitoring the resonance frequencies of single (uncoupled) $L3$ cavities fabricated in the same chip. (d) PL spectra collected from the bulk QDs. (e) Lorentzian fits to the highest frequency modes [shaded in (a), (b), and (c)] to estimate the quality factors. The estimated quality factors for the highest frequency mode in 4, 9, and 16 CCA are ∼1800, ∼2800, and ∼2500, respectively.

We also point out that the number of modes observed in PL should be the same as the number of cavities in the CCA, irrespective of whether the cavities are coupled or not (assuming any degeneracy is lifted due to fabrication imperfection). Without coupling between the cavities, the observed modes would be randomly placed and no specific order between the modes should be observed. On the other hand, in the presence of the coupling between the cavities, the cavity modes are expected to be spaced at a specific order determined by the coupling strengths. However, due to the disorder introduced during the nanofabrication process, the exact distribution of the cavity resonance frequencies will be perturbed. Hence from a statistical study of the differences in the cavity resonance frequencies, we can estimate the ratio between the cavity coupling strengths and the disorder in the cavity resonances. We note that one could instead estimate the disorder in the cavity resonances from the actual cavity frequencies, and not the differences. However, cavities written on different parts of the chip are more susceptible to fabrication variation, and might suffer an overall frequency shift. Thus, the mode separations provide a better measure of the disorder present within each CCA while allowing us to gather statistics from several CCAs for comparison. We have also performed the disorder analysis by using normalized mode separations (normalized by the bare cavity frequency) to exclude any contribution from the overall frequency shift. We found that simple mode separations and normalized mode separations provide very similar results, so in the interests of clarity, we provide statistical data for the actual mode separations only.

III. ESTIMATION OF COUPLING AND DISORDER

Using the coupling strengths derived from FDTD simulations ($t/2\pi = 1.2$ THz, $J_1/2\pi = 0.8$ THz, $J_2 \approx 0$), we calculate the eigenstates of the CCA by diagonalizing the Hamiltonian $\mathcal{H}$:

$$\mathcal{H} = \sum_i \Delta_i a_i^\dagger a_i + \sum_{\langle i,j \rangle} g_{ij}(a_i^\dagger a_j + a_j^\dagger a_i), \tag{1}$$

where Δ_i is the resonance frequency of the ith cavity due to fabrication imperfection, and $g_{i,j}$ is the coupling strength between the ith and jth cavities. The cavity frequencies Δ_i are randomly chosen from a Gaussian distribution with zero mean and standard deviation σ_f:[21]

$$\Pr(\Delta_0) = \frac{1}{\sqrt{2\pi}\sigma_f} e^{-\frac{\Delta_0^2}{2\sigma_f^2}}. \tag{2}$$

The zero for the eigenfrequencies of the coupled-cavity system is set at the frequency of an uncoupled cavity with no disorder. We note that for photonic crystal cavities, the disorder affects both the bare cavity frequencies and the coupling strengths; however, it is very difficult to separate the two effects. Depending on the spatial locations of a disorder, the bare mode separation and the coupling strengths can vary. Figure 3 shows the finite-difference time domain simulation of the effect of disorder on the coupling between cavities in a photonic molecule. We consider two different perturbations in the cavities: in one case, a side hole of one of the cavities is perturbed [Fig. 3(a)], and in the other case, a hole between two cavities is perturbed [Fig. 3(b)]. The unperturbed hole radius is 60 nm, and the perturbed hole radius changes from 30 to 90 nm. We find that the mode separations in the numerically simulated spectrum vary differently [Fig. 3(c)]: for the side hole perturbation, the mode separation changes by ∼500 GHz, whereas for the perturbed hole between two cavities, the mode separation changes by ∼800 GHz. In the latter case, the perturbation affects the coupling strength strongly, but the effect in bare detuning is not significant (as both cavities sense

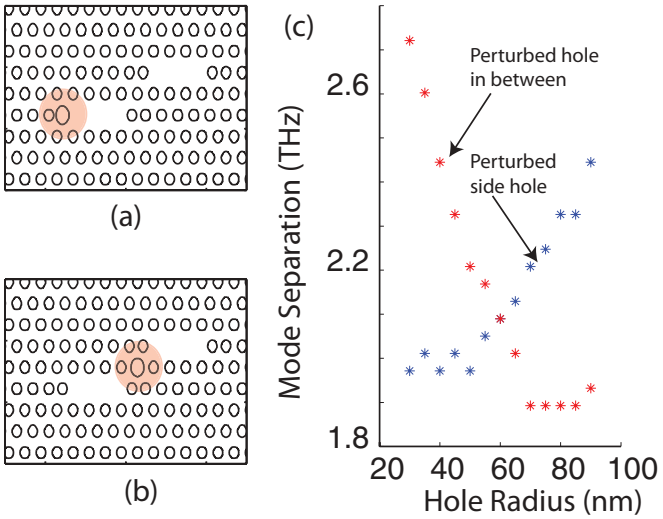

FIG. 3. (Color online) FDTD simulation of the effect of disorder on the observed mode separations in a photonic molecule: (a) perturbation where a side hole in the cavity is changed; (b) perturbation where a hole in between two cavities is changed; (c) the observed mode separations as a function of the perturbed hole radius for two cases shown in (a) and (b). The unperturbed hole radius is 60 nm.

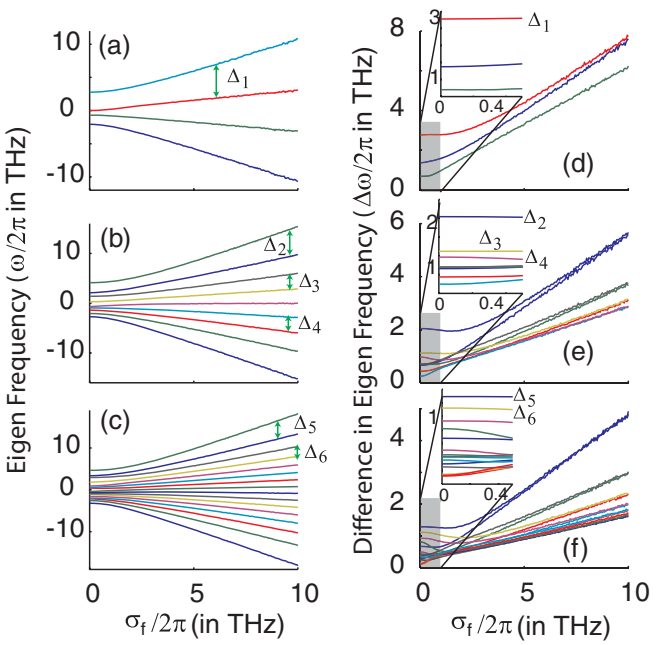

FIG. 4. (Color online) Numerically calculated eigenspectra of the coupled cavities: the eigenfrequencies as a function of the disorder standard deviation σ_f for (a) 4, (b) 9, and (c) 16 cavities in the arrays. The spacings between the cavities are the same as the structures shown in the SEM images in Figs. 1(a)–1(c). The differences in the subsequent eigenvalues are shown as a function of σ_f for (d) 4, (e) 9, and (f) 16 cavities in the arrays. We note that the mode separations increase linearly with increasing σ_f when σ_f is much greater than the coupling strengths, as found in the theory from a simple photonic molecule. Insets magnify the region of low disorder, and we identify the mode separations $\Delta_1 \rightarrow \Delta_6$.

the perturbation). However, for the side hole perturbation, the coupling strength is not affected much, but the bare mode separation changes more. Hence, the experimentally measured variations have contributions from randomness both in the bare mode separations as well as the coupling strengths. Nevertheless, in order to simplify our analysis, we assume that the total variance originates from just the bare mode separations, and the coupling strengths are constant.

The mean values of the eigenfrequencies (averaged over ~10 000 instances) are plotted in Figs. 4(a)–4(c) as a function of increasing σ_f. We observe that the relative separations between the modes follow a specific pattern when the disorder is small. However, with increasing disorder any specific distribution of the cavity modes disappears. This can be observed more clearly in Figs. 4(d)–4(f), where the differences in the mode frequencies are plotted as a function of σ_f. We note that the differences become similar, and increase linearly with σ_f. We note that the mean μ of the mode separations is a combination of the coupling strength and the disorder, whereas the standard deviation σ of the mode separations depends mostly on the disorder. To elaborate further, we can consider the simple example of a photonic molecule (two coupled cavities), where the observed separation Δ between two modes is $\sqrt{\Delta_0^2 + 4J^2}$, with Δ_0 being the random bare detuning between the cavities due to fabrication imperfection and J being the coupling strength.[22] Under the approximation of a Gaussian distribution for the bare cavity detunings, we find that the mean μ of the mode separation Δ (we consider the absolute value of the separation) is $\mu = \sqrt{\frac{2}{\pi}}\sigma_f$ if there is no coupling [$J = 0$ or $\sigma_f/J \gg 1$] and $\mu = 2J + \sigma_f^2/4J + O(\sigma_f^4)$ if the disorder is weak compared to the coupling [i.e., $\sigma_f/J \ll 1$]. The standard deviation σ for the mode separations is $\sigma \sim \sigma_f$ without any coupling ($J = 0$) and $\sigma \sim O(\sigma_f^2/J)$ when $\sigma_f/J \ll 1$. Similar analysis can be performed for CCAs with more than two cavities, although the expressions for the mean and standard deviation become complicated, and a simple closed-form expression is difficult to obtain. Nevertheless, as seen for the photonic molecule, the ratio of the standard deviation to the mean gives us an estimate of the relative contribution of the disorder and the coupling to the mode separations.

We also note that several modes are spaced very closely at weak disorder, indicating a lesser contribution of the coupling to such mode separations [inset of Figs. 4(d)–4(f)]. On the other hand, several detunings between the modes are large compared to others (denoted by $\Delta_1 \rightarrow \Delta_6$), signifying a large contribution from the coupling strengths to the mode separations. We observe that the relative positions of the cavity modes agree qualitatively with our experimental findings. We can identify the same specific separations $\Delta_1 \rightarrow \Delta_6$ between the modes in the experimental results of Fig. 2 as in the theoretical calculations of Fig. 4. Clearly, the fabricated structures are in the regime where the coupling strengths are greater than the disorder. This regime is magnified in the inset of Figs. 4(d)–4(f), and the mode separations $\Delta_1 \rightarrow \Delta_6$ are identified.

IV. STATISTICAL STUDY OF MODE SEPARATIONS

We find a consistent order between the experimentally observed modes of different CCAs (Fig. 2), indicating the

TABLE I. The mean mode separations (μ) and standard deviation (σ) measured over ~30 cavity arrays, with similar hole radii (see Fig. 2 for the definition of the separations).

Δ	μ (THz)	σ (THz)	σ/μ
Δ_1	2.33	0.25	0.1
Δ_2	3.22	0.13	0.04
Δ_3	2.35	0.14	0.06
Δ_4	1.19	0.19	0.16
Δ_5	1.94	0.2	0.1
Δ_6	2.35	0.14	0.06

cavities are coupled. Next we analyze all the separations between the subsequent cavity modes. To do this, we fabricated ~30 copies of each of the three types of cavity arrays, and we calculated the mean μ and standard deviation σ of all these mode separations.

In our fabricated CCAs, we find that the ratio $\sigma/\mu \ll 1$ for almost all the mode separations, indicating the presence of strong intercavity coupling; otherwise, for no coupling, the ratio would be equal to $\sqrt{\pi/2-1} \sim 1$. Table I shows the data for specific separations ($\Delta_1 \rightarrow \Delta_6$) between the cavity modes in the cavity array spectra in detail. We note that all the separations are not equally influenced by the coupling strengths, as seen from the numerical simulations presented above (Fig. 4), and the chosen separations (indicated in Fig. 2) are the ones that are most heavily influenced by the coupling strengths.

Finally, as a further proof of the fact that the detunings between the observed cavity array modes are mostly due to the coupling between the cavities, and not the disorder, we repeated the fabrication of sets of ~30 cavities for different values of air-hole radius for all three types of CCAs. A decreasing trend in the separation is observed with increasing hole radius (Fig. 5). A similar trend is observed in simulation for a photonic molecule with diagonally placed cavities, as a function of the hole radius (inset of Fig. 5). Such a trend also indicates that the separations are mostly due to the coupling between cavities, as a detuning due solely to disorder would have a much weaker dependence on the photonic crystal hole size. The decrease in the mode separation with an increase in the hole radius can be explained by the accompanying increase in the photonic band-gap size (and thus the larger reflectivity of the mirror layers separating cavities, which reduces the cavity couplings).

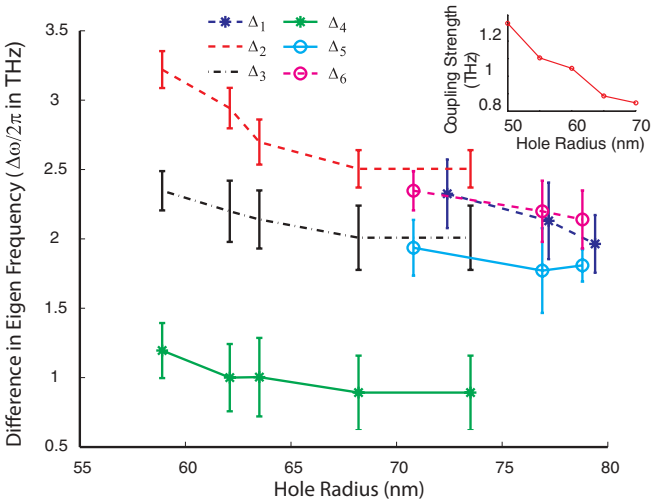

FIG. 5. (Color online) The mode separations $\Delta_1 \rightarrow \Delta_6$ as a function of the photonic crystal hole radius. A decreasing trend in the separation is observed with the increasing hole radius (the photonic crystal lattice periodicity a is 246 nm). For comparison, the inset shows the numerically simulated (FDTD) coupling strength between two cavities placed diagonally as a function of the hole radius.

V. CONCLUSION

We show the signature of large coupling strengths between photonic crystal cavities in a coupled cavity array fabricated in GaAs containing InAs QDs. We observe that the coupling strengths are significantly larger than the disorder introduced during the nanofabrication. Satisfying this condition is necessary for employing such cavity arrays in quantum simulation with correlated photons, although the challenge of achieving a nonlinearity in each cavity still remains open.

ACKNOWLEDGMENTS

The authors acknowledge financial support provided by the Office of Naval Research (PECASE Award, No. N00014-08-1-0561), DARPA (Award No. N66001-12-1-4011), NSF (DMR-0757112), and the Army Research Office (W911NF-08-1-0399). Work at UT-Austin was supported by the Air Force Office of Scientific Research (YIP: FA9550-10-1-0182). A.R. is also supported by a Stanford Graduate Fellowship. This work was performed in part at the Stanford Nanofabrication and University of Texas Microelectronics Research Center facilities of the NNIN, supported by the National Science Foundation.

*arkam@stanford.edu

[1] R. P. Feynman, Int. J. Theor. Phys. **21**, 467 (1982).
[2] M. Greiner, O. Mandel, T. Esslinger, T. W. Hänsch, and I. Bloch, Nature (London) **415**, 39 (2005).
[3] I. Bloch, J. Dalibard, and S. Nascimbène, Nat. Phys. **8**, 267 (2012).
[4] I. Carusotto and C. Ciuti, arXiv:1205.6500v1.
[5] A. D. Greentree, C. Tahan, J. H. Cole, and L. C. L. Hollenberg, Nat. Phys. **2**, 856 (2006).
[6] M. J. Hartmann, F. G. S. L. Brandao, and M. B. Plenio, Nat. Phys. **2**, 849 (2006).
[7] M. Hafezi, E. A. Demler, M. D. Lukin, and J. M. Taylor, Nat. Phys. **7**, 907 (2011).
[8] A. Majumdar, M. Bajcsy, and J. Vučković, Phys. Rev. A **85**, 041801 (2012).
[9] A. Reinhard, T. Volz, M. Winger, A. Badolato, K. J. Hennessy, E. L. Hu, and A. Imamoğlu, Nat. Photon. **6**, 93 (2012).
[10] K. M. Birnbaum, A. Boca, R. Miller, A. D. Boozer, T. E. Northup, and H. J. Kimble, Nature (London) **436**, 87 (2005).
[11] A. Faraon, I. Fushman, D. Englund, N. Stoltz, P. Petroff, and J. Vučković, Nat. Phys. **4**, 859 (2008).

[12]M. Calic, P. Gallo, M. Felici, K. A. Atlasov, B. Dwir, A. Rudra, G. Biasiol, L. Sorba, G. Tarel, V. Savona *et al.*, Phys. Rev. Lett. **106**, 227402 (2011).
[13]A. Huggenberger, S. Heckelmann, C. Schneider, S. Höfling, S. Reitzenstein, L. Worschech, M. Kamp, and A. Forchel, Appl. Phys. Lett. **98**, 131104 (2011).
[14]S. Hughes, P. Yao, F. Milde, A. Knorr, D. Dalacu, K. Mnaymneh, V. Sazonova, P. J. Poole, G. C. Aers, J. Lapointe *et al.*, Phys. Rev. B **83**, 165313 (2011).
[15]A. Surrente, M. Felici, P. Gallo, B. Dwir, A. Rudra, G. Biasiol, L. Sorba, and E. Kapon, Nanotechnology **22**, 465203 (2011).
[16]R. Trotta, A. Polimeni, F. Martelli, G. Pettinari, M. Capizzi, L. Felisari, S. Rubini, M. Francardi, A. Gerardino, P. C. M. Christianen, and J. C. Maan, Adv. Mater. **23**, 2706 (2011).
[17]S. Ferretti and D. Gerace, Phys. Rev. B **85**, 033303 (2012).
[18]I. Carusotto, D. Gerace, H. E. Tureci, S. De Liberato, C. Ciuti, and A. Imamoğlu, Phys. Rev. Lett. **103**, 033601 (2009).
[19]J. Kerckhoff, H. I. Nurdin, D. S. Pavlichin, and H. Mabuchi, Phys. Rev. Lett. **105**, 040502 (2010).
[20]H. Mabuchi, Appl. Phys. Lett. **99**, 153103 (2011).
[21]D. L. Underwood, W. E. Shanks, J. Koch, and A. A. Houck, Phys. Rev. A **86**, 023837 (2012).
[22]A. Majumdar, A. Rundquist, M. Bajcsy, and J. Vučković, Phys. Rev. B **86**, 045315 (2012).
[23]K. A. Atlasov, A. Rudra, B. Dwir, and E. Kapon, Opt. Express **19**, 2619 (2011).
[24]F. Intonti, F. Riboli, N. Caselli, M. Abbarchi, S. Vignolini, D. S. Wiersma, A. Vinattieri, D. Gerace, L. Balet, L. H. Li *et al.*, Phys. Rev. Lett. **106**, 143901 (2011).
[25]M. Galbiati, L. Ferrier, D. D. Solnyshkov, D. Tanese, E. Wertz, A. Amo, M. Abbarchi, P. Senellart, I. Sagnes, A. Lemaitre *et al.*, Phys. Rev. Lett. **108**, 126403 (2012).
[26]S. Vignolini, F. Riboli, F. Intonti, D. S. Wiersma, L. Balet, L. H. Li, M. Francardi, A. Gerardino, A. Fiore, and M. Gurioli, Appl. Phys. Lett. **97**, 063101 (2010).
[27]S. Vignolini, F. Riboli, D. S. Wiersma, L. Balet, L. H. Li, M. Francardi, A. Gerardino, A. Fiore, M. Gurioli, and F. Intonti, Appl. Phys. Lett. **96**, 141114 (2010).
[28]H. Altug and J. Vučković, Opt. Express **13**, 8819 (2005).
[29]H. Altug and J. Vučković, Appl. Phys. Lett. **84**, 161 (2004).
[30]H. Altug and J. Vučković, Appl. Phys. Lett. **86**, 111102 (2005).
[31]A. Danner, J. Lee, J. J. Raftery, N. Yokouchi, and K. Choquette, Electron. Lett. **39**, 311 (2003).
[32]M. Notomi, E. Kuramochi, and T. Tanabe, Nat. Photon. **2**, 741 (2008).
[33]T. Giamarchi, *Quantum Physics in One Dimension* (Oxford University Press, Oxford, 2004).
[34]D. Rossini and R. Fazio, Phys. Rev. Lett. **99**, 186401 (2007).
[35]D. E. Chang, V. Gritsev, G. Morigi, V. Vuletic, M. D. Lukin, and E. A. Demler, Nat. Phys. **4**, 884 (2008).
[36]A. L. C. Hayward, A. M. Martin, and A. D. Greentree, Phys. Rev. Lett. **108**, 223602 (2012).
[37]J. Cho, D. G. Angelakis, and S. Bose, Phys. Rev. Lett. **101**, 246809 (2008).
[38]R. O. Umucalılar and I. Carusotto, Phys. Rev. Lett. **108**, 206809 (2012).
[39]D. Englund, A. Faraon, I. Fushman, N. Stoltz, P. Petroff, and J. Vučković, Nature (London) **450**, 857 (2007).
[40]K. Hennessy, A. Badolato, M. Winger, D. Gerace, M. Atature, S. Gulde, S. Falt, E. L. Hu, and A. Imamoğlu, Nature (London) **445**, 896 (2007).